Paleomagnetic dating of the northern Alberta kimberlites

Vadim A. Kravchinsky, D. Roy Eccles, Rui Zhang, and Matthew Cannon

Abstract: Due to the vast amount of economic interest diamonds have created in northern Alberta, there is a need to produce an accurate geological model for the northern Alberta kimberlite province. To aid in the development of such a model, the emplacement ages of two kimberlite occurrences, K5 and K6 from the Buffalo Head Hills region of north-central Alberta, and the ultramafic Mountain Lake body from northwestern Alberta were estimated using paleomagnetic methods. Paleomagnetic poles obtained in our study do not differ statistically from the reference poles for late Mesozoic – Cenozoic for North America (Besse and Courtillot 2002). With the aid of polarity determinations, palynology, and radiogenic dating, the paleomagnetic results allow for new constraints on the emplacement age of the selected ultramafic occurrences. The paleomagnetic emplacement ages established for the K5, K6, and Mountain Lake bodies are 90–83 Ma, 83.0–79.1 Ma, and not older than 79.1 Ma, respectively.

Résumé : En raison du grand intérêt économique que les diamants ont créé dans le Nord de l'Alberta, il est nécessaire de développer un modèle géologique précis de la province kimberlitique du Nord de l'Alberta. Afin d'aider au développement d'un tel modèle, les âges de la mise en place de deux occurrences de kimberlite, K5 et K6, de la région des collines Buffalo Head du Centre-Nord de l'Alberta et de l'amas ultrabasique Mountain Head du Nord-Ouest de l'Alberta ont été estimés par une méthode paléomagnétique. Les pôles paléomagnétiques obtenus dans notre étude ne diffèrent statistiquement pas des pôles de référence pour l'Amérique du Nord au Mésozoïque tardif – Cénozoïque (Besse and Courtillot 2002). Grâce aux déterminations de polarité, à la palynologie et à la datation radiogénique, les résultats paléomagnétiques limitent l'âge de la mise en place des occurrences ultramafiques sélectionnées. Les âges paléomagnétiques de la mise en place établis pour les amas K5, K6 et Mountain Lake sont respectivement de 90–83 Ma, 83,0–79,1 Ma et pas plus vieux que 79,1 Ma.

[Traduit par la Rédaction]

Introduction

Pioneering work using paleomagnetism on kimberlites was first successfully done in South Africa (Jones 1968). McFadden and Jones (1977) studied five kimberlite pipes to construct the paleomagnetic pole position for Africa in Upper Cretaceous. McFadden (1977) also pioneered the thermoremanence investigation of South African kimberlites and suggested emplacement temperatures of ~300 °C. Since then paleomagnetic dating has been applied in different parts of the world including Canada (Wynne et al. 1992; unpublished report of Enkin (2003) cited by Lockhart et al. 2004). Nevertheless, the technique has not been widely used and our study is the first paleomagnetic study on Alberta kimberlites.

The emplacement temperature of kimberlites is both variable and debated (i.e., Van Fossen and Kent 1993). Some authors argue in favor of a "cold" emplacement temperature, which would limit the overprinting effects, but other cases of kimberlite related remagnetization (thermochemical) could also occur. Watson (1967), Mitchell (1986), and Skinner and Marsh (2004) proposed intrusion temperatures of <500 °C for volcaniclastic kimberlites based on the common absence of thermal metamorphic indications in xenoliths and in adjacent country rock. Sosman (1938) (cited in Watson 1967) studied the thermal effects of North American kimberlite on coal inclusions and derived a temperature of 340 °C. Stability fields of alteration assemblages in kimberlite pyroclastic rocks gave a lowest temperature constraint of 300–340 °C (Stripp et al. 2006). Recently, Fontana et al. (2008) demonstrated that two different neighbouring kimberlite pipes in South Africa had emplacement temperatures of ≤340 °C and 260 to >590 °C, supporting earlier published data on various emplacement temperature ranges for different petrologic and tectonic conditions.

The first hint of diamond potential in Alberta occurred in 1958, when Mr. Einar Opdahl discovered a 0.83 carat octahedral alluvial diamond on his farm north of Evansburg. In 1990, Monopros Limited (then the Canadian exploration subsidiary of De Beers) discovered two non-archetypal kimberlites located directly north of Mountain Lake in northwestern Alberta, ~75 km northeast of Grande Prairie (Fig. 1). However, it was not until the early to mid 1990s that diamondiferous kimberlites were discovered in northern Alberta (Eccles et al. 2003).

Forty-eight occurrences of ultramafic (non-archetypal kimberlite) to kimberlite rocks are known to exist in three

Received 24 July 2008. Accepted 8 April 2009. Published on the NRC Research Press Web site at cjes.nrc.ca on 15 May 2009.

Paper handled by Associate Editor F. Cook.

V.A. Kravchinsky,[1] R. Zhang, and M. Cannon.[2] Physics Department, University of Alberta, Edmonton, AB T6G 2G7, Canada.
D.R. Eccles. Energy Resource Conservation Board, Alberta Geological Survey, 4th Floor Twin Atria Building, 4999 - 98 Avenue, Edmonton, AB T6B 2X3, Canada.

[1]Corresponding author (e-mail: vkrav@phys.ualberta.ca).
[2]Present address: Shell Canada Limited, 400 - 4th Avenue, Calgary, AB T2P 0J4, Canada.

separate areas of northern Alberta: the Mountain Lake ultramafic cluster, and the Buffalo Head Hills and Birch Mountains kimberlite fields (Fig. 1). These occurrences collectively define the northern Alberta kimberlite province (Eccles et al. 2003, 2004). The area with the best diamond results, the Buffalo Head Hills kimberlite field, is ~390 km north of the city of Edmonton and consists of 40 kimberlites of which 27 contain diamonds (Fig. 1).

The Precambrian basement rocks in the Buffalo Head Hills and Mountain Lake areas are overlain by thick sequences that are composed of Cretaceous clastic sediments overlaying Devonian carbonates. The total thickness of sediments is ~1500 m for the Buffalo Head Hills and 2600 m for Mountain Lake area. The uppermost sedimentary units are Early and Late Cretaceous (100 to 80 Ma) sediments of the Western Canada Sedimentary Basin.

To produce an accurate geological model of the northern Alberta kimberlite province, an accurate assessment of emplacement ages is required. Prior to this study, the emplacement age of several kimberlitic occurrences were determined using U–Pb perovksite and Rb–Sr phlogopite radiogenic techniques (Skelton et al. 2003; Heaman et al. 2004; Eccles 2004; Eccles et al. 2008) and palynological determinations (Leckie et al. 1997; Wood et al. 1998; Sweet et al. personal communication, 2008). Collectively, the Mountain Lake ultramafic cluster and the Buffalo Head Hills and Birch Mountains kimberlite fields in northern Alberta were emplaced during a 28 million year period spanning Late Cretaceous to Paleocene (~88 to 60 Ma; Eccles et al. 2008). Unfortunately, Alberta kimberlites do not always contain mineral suites suitable for U–Pb dating (e.g., perovskite, ilmenite) or, in many cases, these minerals may be too small to separate and pick with any certainty. Thus, the paleomagnetic technique used here is similar to an orientation study where paleomagnetic results could be assessed versus robust U–Pb emplacement ages.

The size of the kimberlite bodies, as gathered from aeromagnetic survey data and drilling, varies from <1 to ~45 ha (Eccles et al. 2004). Sediments of a few dozen metres thickness usually cover the kimberlites. Only a few bodies crop out, including the three exposures studied here. Pyroclastic kimberlitic rocks are by far the dominant textural rock type in the northern Alberta kimberlite province, followed by less common resedimented volcaniclastic kimberlitic rocks (Eccles et al. 2004).

The Mountain Lake kimberlites do not have classic kimberlite geochemical signatures, and mounting evidence, which includes major and incompatible element patterns, high-Al clinopyroxene, and trend 2-type spinels, classifies the Mountain Lake kimberlite occurrence as alkaline basalt (Eccles et al. 2004). The Buffalo Head Hills kimberlite field resembles Group I South African kimberlite (Eccles et al. 2004). The Group I kimberlites are essentially phlogopite free, have unradiogenic Sr and radiogenic Nd isotope ratios relative to present-day typical compositions, and have been recorded from most continents, occurring within Archean and Proterozoic terranes. The two studied bodies, referred to as K5 and K6, are composed primarily of pyroclastic kimberlitic rock with juvenile lapilli-bearing olivine tuff infilling and contain a moderate amount of mantle xenoliths of small sizes (usually <1 mm).

We applied the paleomagnetic technique to provide another dating methodology applicable to three exposed kimberlitic bodies. The K5 and K6 kimberlites from Buffalo Head Hills and the ultramafic body at Mountain Lake were examined in this first paleomagnetic study of Albertan kimberlitic rocks. In addition, Late Cretaceous (Campanian) Wapiti Group sandstone was sampled directly adjacent (a few dozen metres) to the Mountain Lake body in bedrock exposed by the Mountain Lake Creek to determine the polarity of the area.

Methods

We sampled 2.5 cm diameter cores, using a portable drilling apparatus with a water-cooled diamond bit. The orientation of the cores was determined using an orientation stage with a magnetic compass and inclinometer. The cores were cut in the laboratory into cylindrical or half-cylindrical samples 0.8–2.2 cm long. Most studied samples contained no large xenoliths (commonly <1 mm) in the main matrix; only a few samples in K6 had 3–5 mm size inclusions. Country rock xenoliths are composed of shale and carbonate; mantle xenocrysts are primarily olivine and serpentine with some accessory minerals (chromite, perovskite, apatite, magnetite, and ilmenite).

Margins of the kimberlite occurrences were not exposed and so samples were taken closer to the centres of the studied bodies, where maximum emplacement temperature responsible for the acquisition of the thermoremanent magnetization would be expected. Size of the outcrops was from a few metres (K6) to 30–40 m (K5) and tended to be near the centre of the kimberlite occurrence. The sizes of the bodies themselves are relatively large, approximately 750 m × 600 m and 450 m × 600 m, respectively, for K5 and K6. The Mountain Lake occurrence forms a pronounced topographic high and measures at least 400 m × 650 m (total of 29 ha) (Eccles et al. 2004).

Magnetic measurements and demagnetization procedures to identify the magnetic minerals, isothermal remanent magnetization (IRM) acquisitions, and temperature dependant magnetic susceptibility were performed in the magnetically shielded room of the paleomagnetic laboratory at the Department of Physics, University of Alberta. Remanent magnetization measurements were carried out using a Molspin spinner magnetometer and 2G Enterprises superconducting horizontal magnetometer. Hysteresis loops and low-temperature scans were done on a few specimens using the Physical Property Measuring System (manufactured by Quantum Design) at the Department of Chemistry, University of Alberta. Unblocking and blocking temperatures, determined from thermomagnetic susceptibility curves, were measured with a Bartington susceptibility meter system in the air.

Laboratory demagnetization measurements were performed at the Physics Department of the University of Alberta. Twenty-two specimens were thermally demagnetized over 19 temperature steps up to 590–690 °C in a nonmagnetic oven placed within a permalloy shielded room with 8 nT residual magnetic field. The mineralogical changes during heating were monitored by measuring magnetic susceptibility after each incremental temperature step. During

Fig. 1. Geological setting of northern Alberta with the location of ultramafic to kimberlite occurrences in the Mountain Lake, Buffalo Head Hills, and Birch Mountains fields. Inferred basement tectonic domains (left) are from Ross et al. (1994) and bedrock geology (right) is from Hamilton et al. (1999). Bedrock acronyms Ksh, Ks, and Kd reference Cretaceous (Albian to Santonian) bedrock units: Shaftesbury Formation (shale and silty shale), Smoky Group (shale and silty shale), and Dunvegan Formation (sandstone), respectively. GSLSZ, Great Slave Lake Shear Zone; STZ, Snowbird Tectonic Zone.

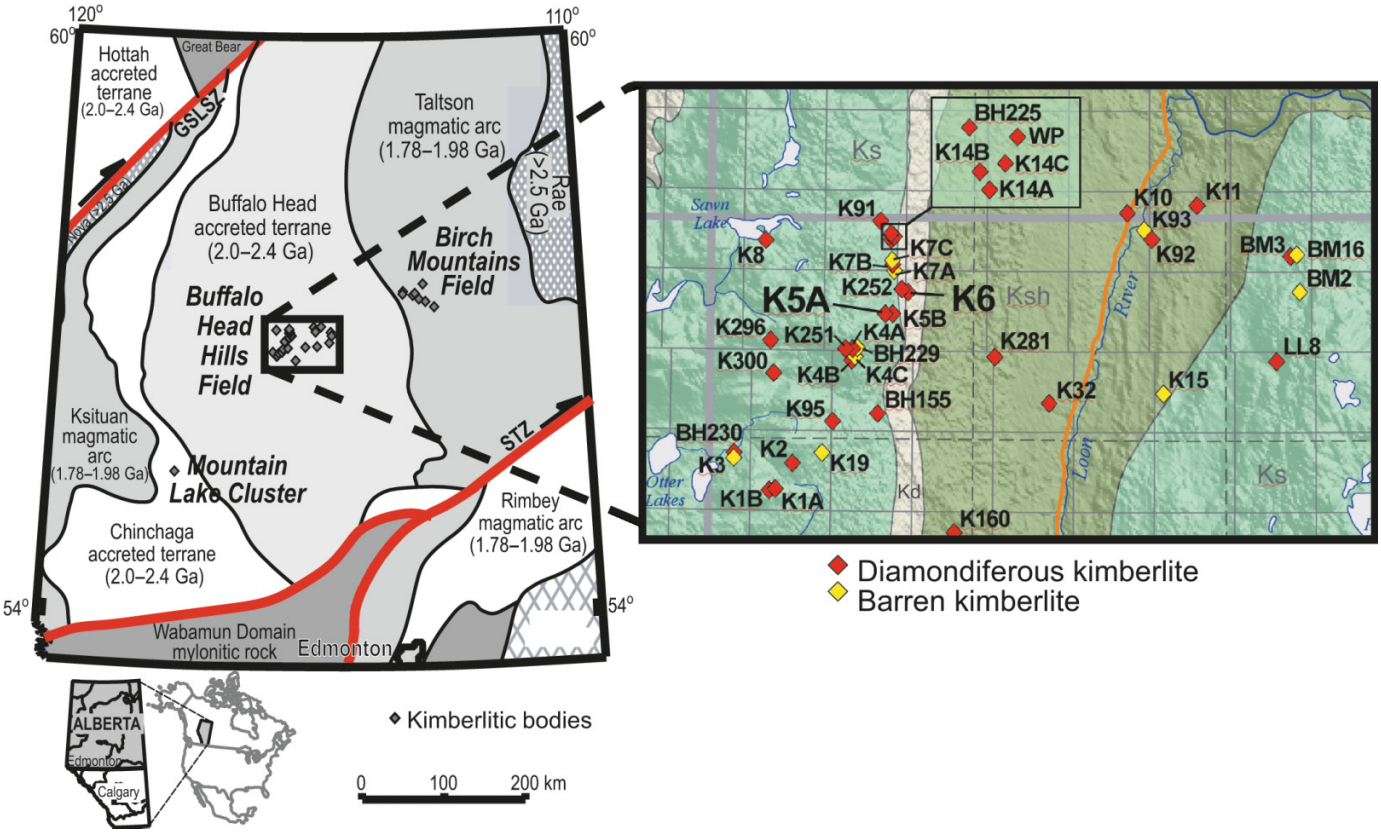

thermal demagnetization, sample orientation was successively inverted about the *z*-axis to detect any systematic magnetization that could have resulted from the small 6 nT residual magnetic field in the furnace placed in the permalloy shielded room. Alternating field (AF) demagnetization was conducted on 54 samples over 14 incremental steps up to 100 mT.

Overall, 67 of 76 samples demonstrated comprehensible behavior during demagnetization experiments. Demagnetization results were plotted as orthogonal vector diagrams (Zijderveld 1967) and as equal-area projections. Both paleomagnetic directions were determined using principal component analysis (Kirschvink 1980) or remagnetization great circles (Halls 1976; McFadden and McElhinny 1988). Site-mean directions were calculated using Fisher (1953) and McFadden and McElhinny (1988) statistics for combined directional data and great circles. All interpretations and data processing were carried out using the PaleoMac software (Cogné 2003).

Paleomagnetic results

Magnetic minerals

Results of the experiments on magnetic mineralogy assessment are shown in Figs. 2, 3, and 4 with representative specimens chosen for each kimberlitic body. Although the IRM acquisition curves are different for all three kimberlite bodies, all specimens generally reveal a behavior characterized by a low coercivity over a large range 0.1–1.0 T (Fig. 2). In this experiment, samples were first demagnetized and then saturated in a progressively stronger applied field before being gradually reduced to zero in the backfield direction. All K6 samples were saturated in an applied field of <250 mT (Fig. 2; Table 1), suggesting that the main ferromagnetic mineral is magnetite (Dunlop and Özdemir 1997). Samples of kimberlite bodies K5 and ML have saturation above 600 mT, indicating that the main mineral carrier of remanent magnetization for both of these occurrences is titanomagnetite.

Dankers (1981) provides important parameter references for a number of artificial rock specimens with well-defined 5–250 μm natural magnetite, titanomagnetite, and hematite. The remanent acquisition coercive force (H'_{cr}) over the remanent coercive force (H_{cr}) ratio is used here to differentiate magnetite and titanomagnetite. Kimberlite samples in our study yield H'_{cr}/H_{cr} = 1.22 ± 0.04 for K5, 1.16 ± 0.07 for ML, and 1.67 ± 0.17 for the K6 pipe (Table 1). Following Dankers' study, H'_{cr}/H_{cr} = 1.6 ± 0.2 is typical for pure magnetite and H'_{cr}/H_{cr} = 1.2 ± 0.2 for titanomagnetite. Therefore, we reiterate that the main carrier of the natural remanent magnetization (NRM) in K5 and Mountain Lake is titanomagnetite and in K6 is magnetite. The hysteresis of pilot samples from K5 and K6 (Figs. 3*a*, 3*b*) confirms the pres-

Fig. 2. Isothermal remanent magnetization (IRM) for representative specimens from the studied kimberlites.

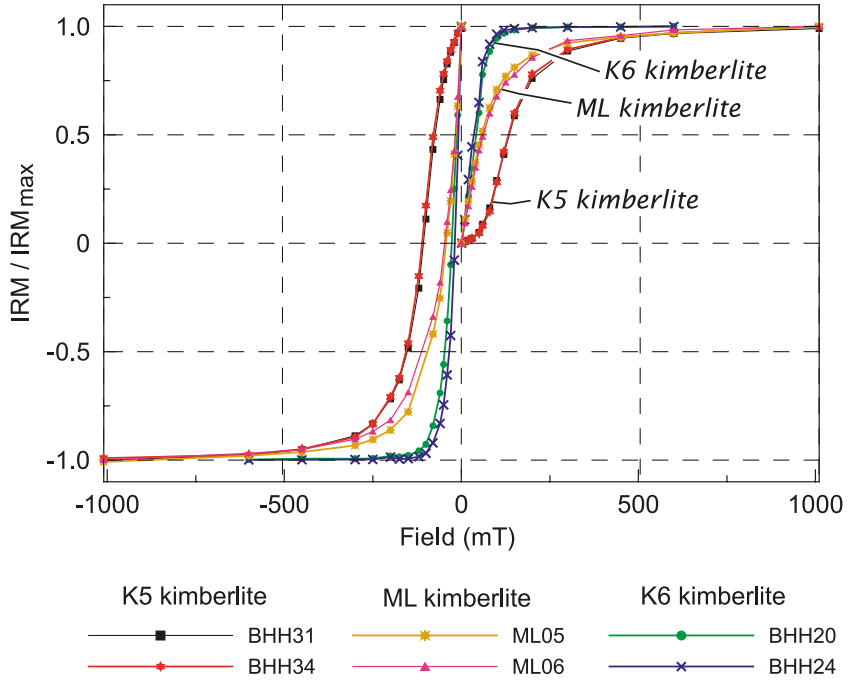

ence of the low-coercivity minerals (Dunlop 2002). Two measured K5 samples fall into single-domain magnetic grain-size category, and K6 samples are in the pseudo-single – multi-domain cluster (Fig. 3*c*).

Although the susceptibility versus temperature curves are generally not reversible due to heating induced alterations, they show a sharp drop of the susceptibility at about 560–580 °C for the K6 sample BHH24 in Fig. 4. Additionally, the Verwey transition is clearly observed at 114–124 K from the low-temperature susceptibility measurement (sample BHH01, Fig. 4), as expected for magnetite (Dunlop and Özdemir 1997). Both results are diagnostic for the presence of magnetite with diminutive titanomagnetite content in the kimberlite pipe K6.

High-temperature magnetic susceptibility data also support a Fe-rich titanomagnetite magnetic mineralogy conclusion for K5 and ML. The lower Curie point (~350 °C) from sample BHH32 (Fig. 4) indicates a larger Ti content. Increasing the temperature of this sample above 350 °C leads to the oxidation of titanomagnetite forming new magnetic minerals, as indicated by an increase in the magnetic susceptibility.

Our analysis of magnetic minerals demonstrates that ML and K5 have titanomagnetite and K6 has magnetite as main carriers of remanent magnetization, even though K5 and K6 are situated in the same area, the Buffalo Head Hills kimberlite field. K5 and K6 also have different grain sizes of magnetic minerals. The discrepancy could be caused by the difference in the magma sources.

Figure 5 shows typical behavior of the samples during the thermal demagnetization. The magnetic susceptibility was monitored after each heating step to examine mineralogical changes during the experiment. The susceptibility is relatively high and does not change significantly for sample BHH22A; however, samples BHH03A and BHH07 show significant increase in susceptibility over 525 °C, indicating that magnetization measurements above this temperature could not be used for further directional analysis. Every studied kimberlite body has samples with higher and lower susceptibility. The magnetic susceptibility value is quite diverse for different samples from the same kimberlite site and depends on the concentration of magnetite grains in each particular sample.

Paleomagnetism of the K5 kimberlite

Based on radiogenic age determinations, a single fraction of red-orange perovskite cubes was analyzed from a sample of the K5A kimberlite. These grains have moderate U (68 ppm) but low Th (175 ppm) and Th/U (2.6), with a model $^{206}Pb/^{238}U$ age of 87.6 ± 4.6 Ma interpreted as the best estimate for the emplacement age of the K5A kimberlite (Skelton et al. 2003; Heaman et al. 2004; Eccles et al. 2008).

Both thermal and AF demagnetizations applied to the K5 kimberlite samples demonstrated the presence of two components. The low-field or low-temperature component (LTC) was usually demagnetized above 200 °C and 20–30 mT (Fig. 6). The average LTC direction of 11 samples from K5 is declination (D) = 24.2°, inclination (I) = 21°, with precision parameter (k) = 2.5; confidence cone radius (α_{95}) = 37.0° (Fig. 7; Table 2). However, the data are scattered and do not coincide with the direction of the present geomagnetic field (PGF) or axial dipole direction (AD) in the sampling region (D_{PGF} = 19.6°, I_{PGF} = 77.6°, I_{AD} = 71.9°), nor with the mean high-temperature (or high-field) component (HTC) of other studied kimberlites (see Table 2). The LTC scatter might be caused by a later overprint during long-term exposure to the reversal polarity geomagnetic field or be a signature of the partial overprint caused by a later tectonic process if some low-temperature reheating was involved. A very low value for k and a high value of

Fig. 3. Hysteresis loops from (A) K5 and (B) K6 kimberlite. Insets illustrate the original measure before correction for the paramagnetic effect was applied. (C) Hysteresis parameter plot for four K5 and K6 samples. *M*, magnetization (in amperes per metre); *H*, applied magnetic field intensity (in tesla); SD, single-domain particle region; PSD, pseudo-single domain; MD, multi-domain particle region.

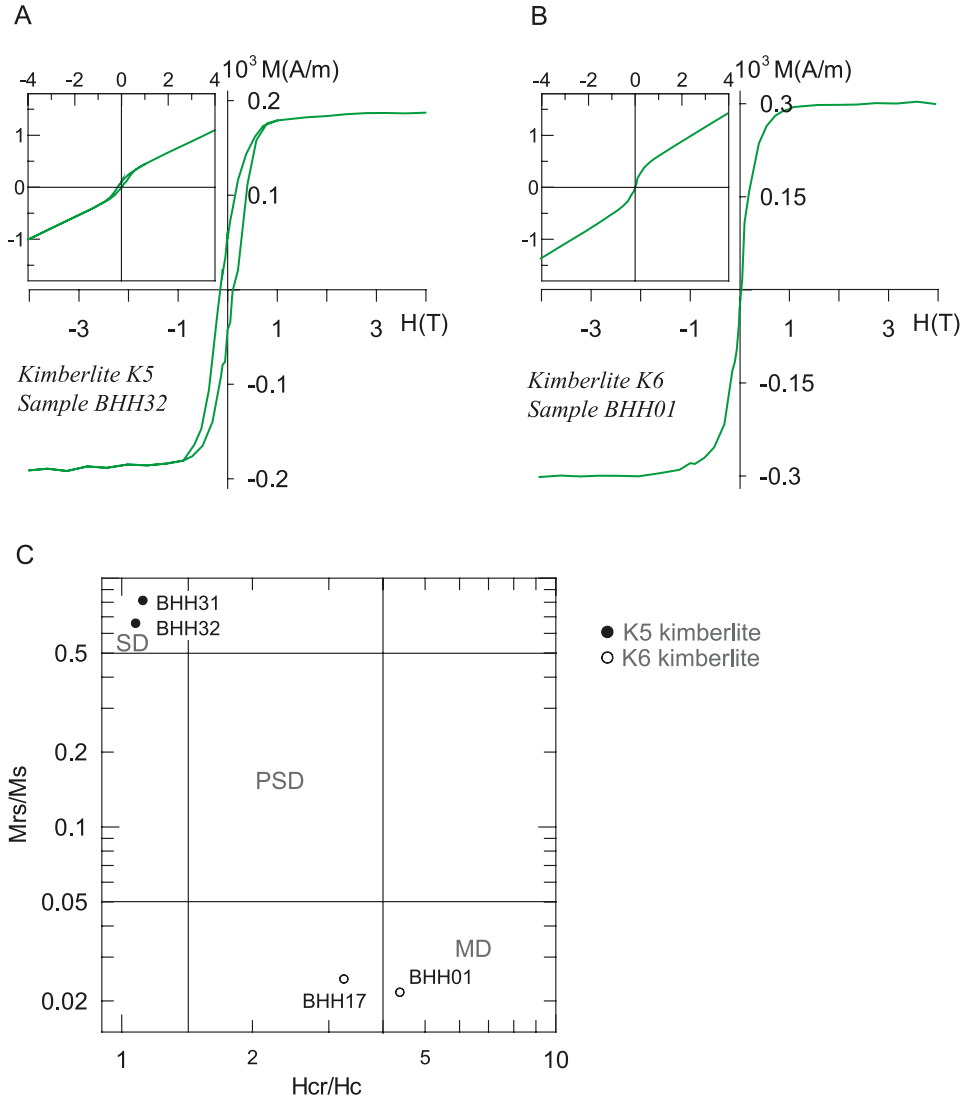

α_{95} support the possibility of the incomplete overprint genesis of the LTC.

Alternatively, the LTC scatter might be caused by a partial remagnetization of the xenoliths in kimberlites. If emplacement temperature of kimberlite was below the blocking temperature, it could only partially overprint the original magnetization of the xenoliths. In such case, xenoliths could show the presence of both low- and high-temperature components. The scattered LTC could signify that various inclusions could have been remagnetized during the magma emplacement at the different rate. We compared demagnetization results of the samples with different sized xenoliths (from <1 to 3–5 mm diameter) and did not find any difference in their behavior. The HTC was found in all samples, which enables us to conclude that the thermoremnant magnetization acquired during kimberlite formation was quite strong and emplacement temperatures have not been too low.

Figure 6 demonstrates that the HTC could be observed between 30 and 90 mT and 200–500 °C and that thermal and AF demagnetizations show similar results; two specimens from the same sample (BHH30) demonstrate a similar demagnetization pattern. All HTC directions group together closely around a steep positive mean direction (D = 355.4°, I = 76.3°) with high precession parameter (k = 57.1) and low 95% confidence cone radius (α_{95} = 4.5°).

Paleomagnetism of the K6 kimberlite

Eccles (2004) reported an "approximate" radiogenic $^{206}Pb/^{238}U$ perovskite age for the K6 body of 91.9 ± 2.0 Ma. This is not a robust determination because of low U (19.9 ppm) and a low $^{238}U/^{204}Pb$ ratio compared with typical kimberlite perovskite. While Eccles (2004) recommends further analyses be completed to determine a more robust radiogenic age for K6, we include this value only as a proxy for a comparison with paleomagnetic ages determined in this study.

The LTC for K6 is detected in ~60% of all demagnetized samples and can be removed at 15–20 mT during the

Fig. 4. High and low temperature scan for magnetic susceptibility. Only heating is shown. All heating curves are not reversible. Note that the low-temperature scan is in K (kelvin).

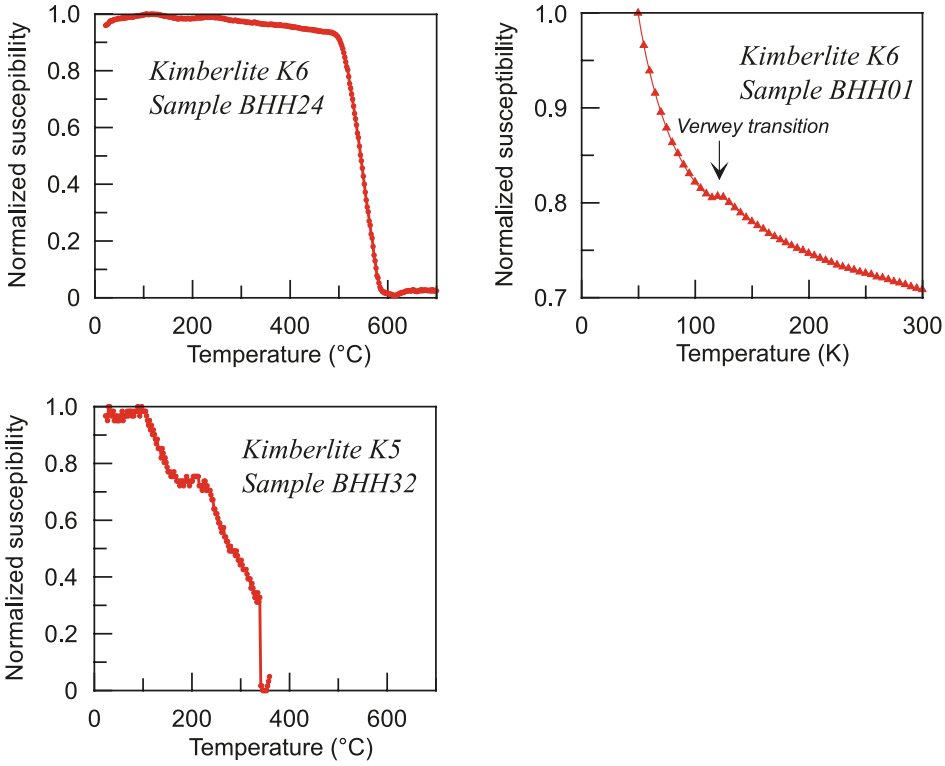

Table 1. Results of the IRM experiment.

Ultramafic body	Sample No.	Coercive force H'_{cr} (mT)	Remnant coercive force H_{cr} (mT)	H'_{cr}/H_{cr}	Saturation magnetization (10^{-5}A/m)	Saturation field (mT)
K5	K29	133	112	1.19	100.5	650–1000
	K31	132	113	1.17	98.5	550
	K31a	136	106	1.28	27.71	510
	K32a	130	106	1.23	45.68	600
	K34	139	116	1.20	70.4	650–1000
	K36	150	118	1.27	39.5	650–1000
K5 average				1.22±0.04		
K6	K01	35	23	1.52	182.3	250
	K17	37	24	1.54	95.73	125
	K17a	39	26	1.5	169	175
	K20	40	23	1.74	47.4	150
	K24	34	18	1.89	125	120
	K27	46	25	1.84	261	140
K6 average				1.67±0.17		
Mountain Lake	ML03	85	73	1.16	14.96	~1000
	ML05	55	50	1.1	14.5	800
	ML06	61	55	1.11	9.71	650
	ML07	70	56	1.25	5.89	~1000
ML average				1.16±0.07		

AF experiment or at 150–180 °C during the thermal demagnetization (Fig. 8). Some samples (~40%) do not have the LTC (e.g., sample BHH22A). The HTC, however, cannot be resolved for some samples completely even at high fields and temperatures. Sample BHH06A represents the samples in which the LTC removed at 20 mT, but applied fields above 30 mT caused the direction to scatter chaotically, while the NRM intensity approached zero. However, we can easily observe the track of the NRM during demagnetization as the positive direction of the LTC as it moved towards the HTC along a great circle. The mean LTC direction evaluated for 20 samples is $D = 344.4°$, $I = 72.2°$ ($k = 14.2$, $\alpha_{95} = 9.0°$) (Fig. 7; Table 2), which is close to the present-day field (PDF) expected direction in the area $D_{PDF} = 19.2°$, $I_{PDF} = 77.7°$. Hence, we interpret the LTC as a Brunhes chron overprint. The LTC cluster in Fig. 7 has

Fig. 5. Magnetic susceptibility monitored after each thermal demagnetization step. Dramatic increase of magnetic susceptibility above 525 °C for samples BHH07 and BHH32 signifies the change in magnetic minerals during heating (oxidation of magnetite converting it to hematite). Demagnetization steps that corresponded to the augmented magnetic susceptibility were eliminated from the analysis.

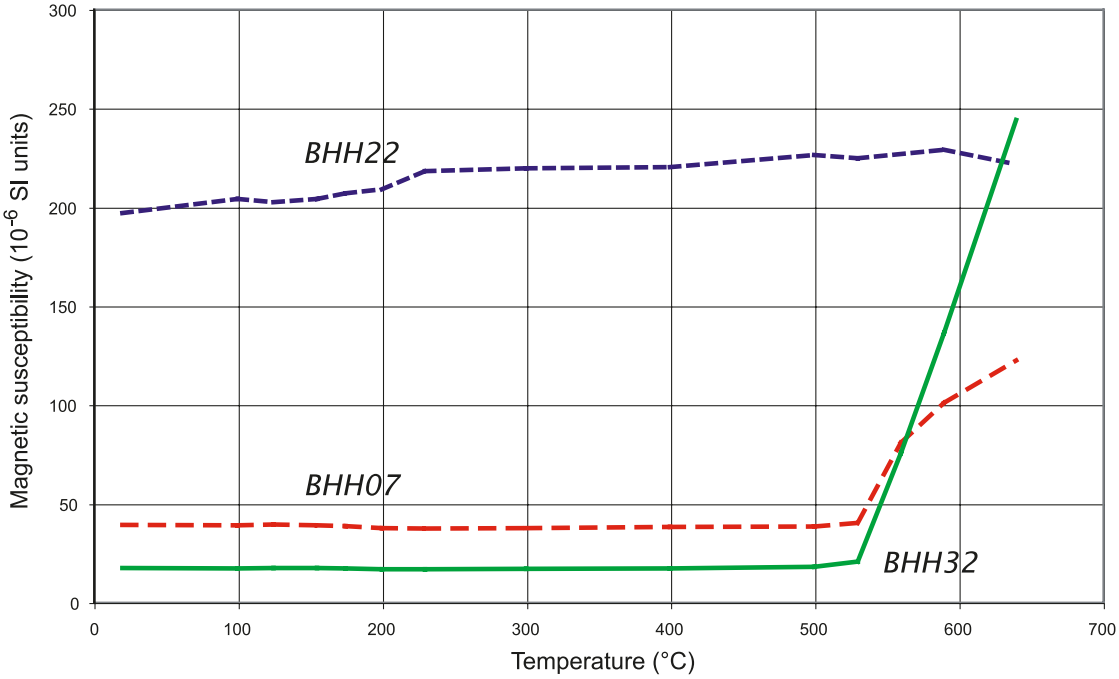

quite an elongated shape; it could be the result of the incomplete separation of the HTC and LTC during the demagnetization experiment.

The HTC was evaluated using the remagnetization circle technique for half of the samples (Halls 1976). Sample BHH06A illustrates typical behavior during the demagnetization experiment, when demagnetization steps form a trace along the great circle but do not reach a stable HTC direction. The other half of the samples have a stable single-component direction with negative inclination. Three samples (BHH07A, BHH07TA, and BHH22A) in Fig. 8 have similar HTC using different demagnetization techniques. Samples BHH07A and BHH07TA are representative of AF and thermal demagnetization for the same oriented core. Although the HTC directions have negative inclinations, there is a notable difference in declination. Sample BHH22A also has negative albeit shallower inclination. We presume that such differences could be caused by incomplete separation of the low- and high-temperature components and the relatively weak nature of the HTC. Eighteen samples can be examined only by great circles and 15 samples by the HTC directions (Fig. 7; Table 2). First, the mean paleomagnetic direction for K6 was calculated by combining directions and great circles (McFadden and McElhinny 1988). The directions are considerably scattered and elongated along the great circle of remagnetization connecting the LTC and HTC mean directions. The average direction is $D = 173.4°$, $I = -70.7°$ for combined analyses (directions and circles) with acceptable statistical parameters due to the high number of samples used for calculation ($k = 10.9$, $\alpha_{95} = 7.9°$). The method, however, works well when one component is highly dispersed compared to the other; therefore, we calculated a mean direction without using circles: $D = 163.8°$, $I = -75.3°$ ($k = 12.2$, $\alpha_{95} = 11.4°$) (Table 2). The confidence cone radius is slightly higher but the direction itself is more correct compared with the combined directions and circles technique. The only direction mean is located closer to the expected direction for the Upper Cretaceous reversal polarity interval at 80 Ma of Besse and Courtillot (2002) ($D = 160.0°$, $I = -80.3°$, $\alpha_{95} = 6.9°$).

Paleomagnetism of the Mountain Lake ultramafic body

Palynologies of nonmarine sedimentary clasts were used by Wood et al. (1998) to infer a maximum emplacement age of mid-Maastrichtian, probably ca. 68 Ma. Leckie et al. (1997) reported that in situ laminated sediments, which they interpreted to be interbedded with volcaniclastic deposits and mudstone clasts, have a palynological assemblage that is similar to the Dinosaur Park Formation and are late upper Campanian in age (between ca. 75 and 76 Ma). Three samples of sandstone from MLN (drill core ML95-1) were processed for apatite fission track (AFT) dating. The central AFT ages range from 78 ± 9 Ma to 72 ± 7 Ma (Leckie et al. 1997). To summarize, the existing data indicate the emplacement age for the Mountain Lake pipes is late Late Cretaceous, or between about 76 and 68 Ma.

Mountain Lake sampling was limited to eight cores because the highly fractured, brittle ultramafic rock made drilling or taking oriented hand-blocks difficult. Three demagnetization samples (ML02C, ML02T, and ML07B) illustrate the presence of one or two components (Fig. 9A). Samples ML02C and ML02T were cut from the same core and demagnetized with AF (ML02C) or temperature (ML02T). Both treatments demonstrated a similar result. Sample ML07B demonstrates LTC that does not fit with the present-day overprint. The situation is very similar to the K5 body, where the LTC has a scattered shallow positive, with some negative, inclinations (Fig. 7). The mean direction for

Fig. 6. Results of alternating field and thermal demagnetization for K5 kimberlite samples. Typical equal-area projections illustrating demagnetization paths during experiments (top) and demagnetization orthogonal vector plots (Zijderveld 1967). Closed or open symbols in orthogonal plots are projections onto the horizontal or vertical plane, respectively; temperature steps are indicated in °C. Least square best-fit lines are shown for the low-temperature (low-field) component (LTC) at the orthogonal plots; LTC directions corresponding to the best-fit lines in the orthogonal plots are shown as a star in the equal-area projections. All in situ coordinates. NRM, natural remanent magnetization.

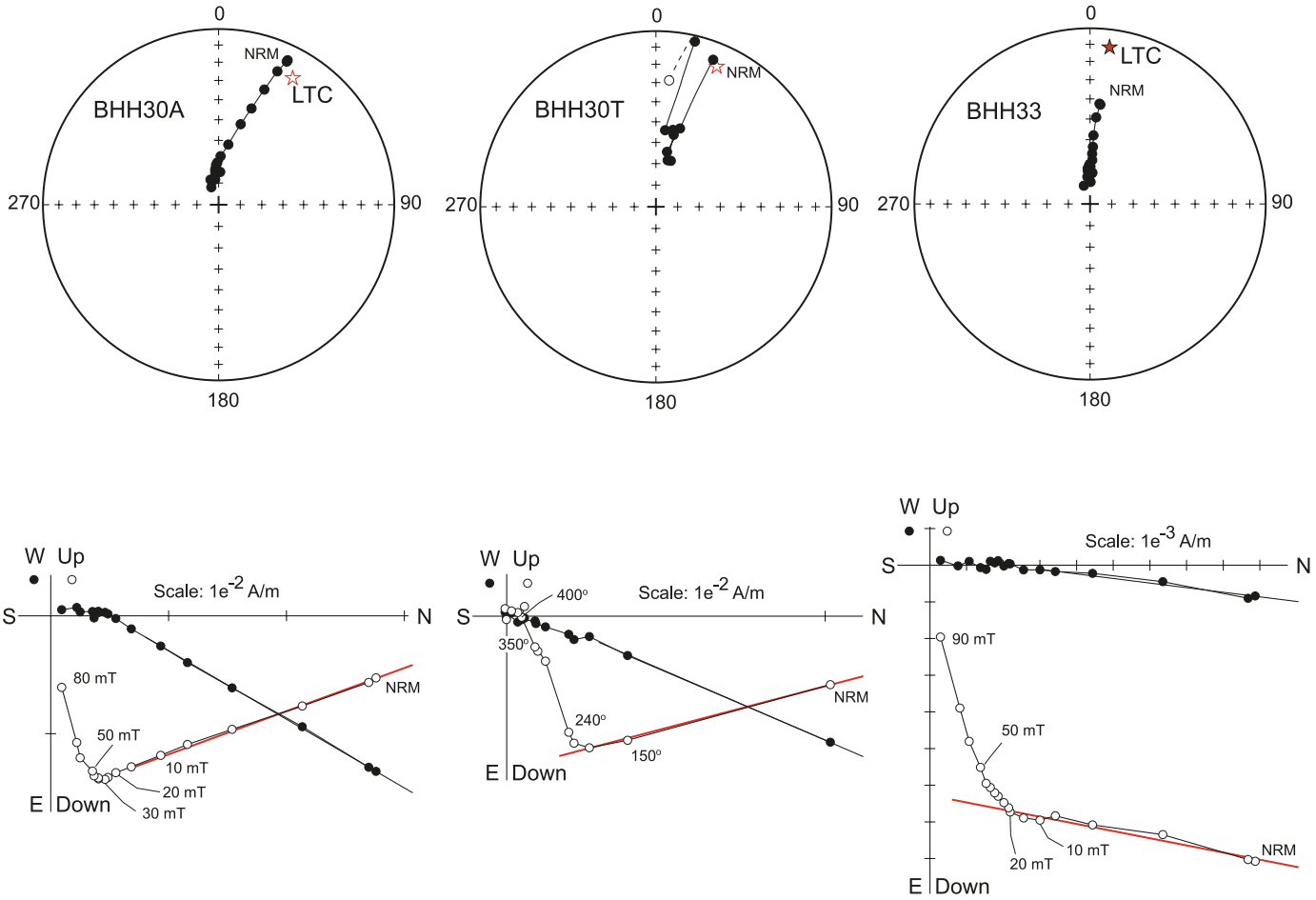

the LTC of 11 samples is $D = 314.4°$, $I = 26.4°$. Statistic parameters ($k = 4.9$, $\alpha_{95} = 23.0°$) demonstrate large scatter that could signify incomplete separation of the LTC from the HTC.

It was possible to evaluate the high-temperature field component in all Mountain Lake samples. The component has positive steep inclination with noticeable scatter. Mean direction for HTC is $D = 264.0°$, $I = 68.2°$ ($k = 14.3$, $\alpha_{95} = 10.5°$) and does not fit the PDF direction. We consider this a preliminary estimation because of the small number of samples (15 samples from eight cores) and the fractured nature of rocks at the sampling site. In addition, we cannot rule out some amount of displacement of the ultramafic outcrop rock at Mountain Lake during excavation that would result in inaccurate core orientation. However, it is worth mentioning here that a clockwise rotation of the LTC directions' mean by 70° would bring it into agreement with the LTC found in K5 kimberlite and would also make the HTC have a more likely $D = 334°$, $I = 68°$ direction, which is much closer to the expected direction of Besse and Courtillot (2002) for 80–70 Ma. Chen and Olson (2005) reviewed a number of the post-Late Cretaceous, large-scale tectonic processes, and we consider that some of them might be responsible for such remarkable rotation of Mountain Lake area relatively to Buffalo Head Hills, although we consider such tectonic explanation of the 70° rotation as very preliminary. The oblique collision of accreting terranes in the west of the study area that took place from Middle Cretaceous to Middle Eocene created the tectonic displacement of crustal rocks on the continental margin of North America (Price 1994). Early Tertiary compressional and strike-slip structures activated the older rift-related features in the region (Dixon 1993). In the Eocene, convergence of tectonic processes in the Rocky Mountains terminated and, consequently, subsidence and filling of the foreland sedimentary basin ended (Armstrong 1993). In the Early and Middle Eocene crustal extension in the central part of the Cordillera tectonically reshaped the foreland basin producing a pattern of thrusts and fold belts (Price 1994).

Figure 9B illustrates demagnetization of the Late Cretaceous Wapiti Group sandstone that hosts and is located directly adjacent to the geophysical outline of Mountain Lake. The orientation of these samples was not very precise because of the complex sampling procedure used for unconsolidated bedrock in the field; only eight samples were taken

Fig. 7. Equal-area projection of site-mean direction of the low-temperature (LTC) and high-temperature (HTC) magnetization component for the K5, K6, and Mountain Lake kimberlites. Closed or open symbols show downward or upward inclinations, respectively. Star, mean direction with 95% confidence zone. All in situ coordinates. *D*, declination; *I*, inclination; *k*, precision parameter; α_{95}, confidence cone radius.

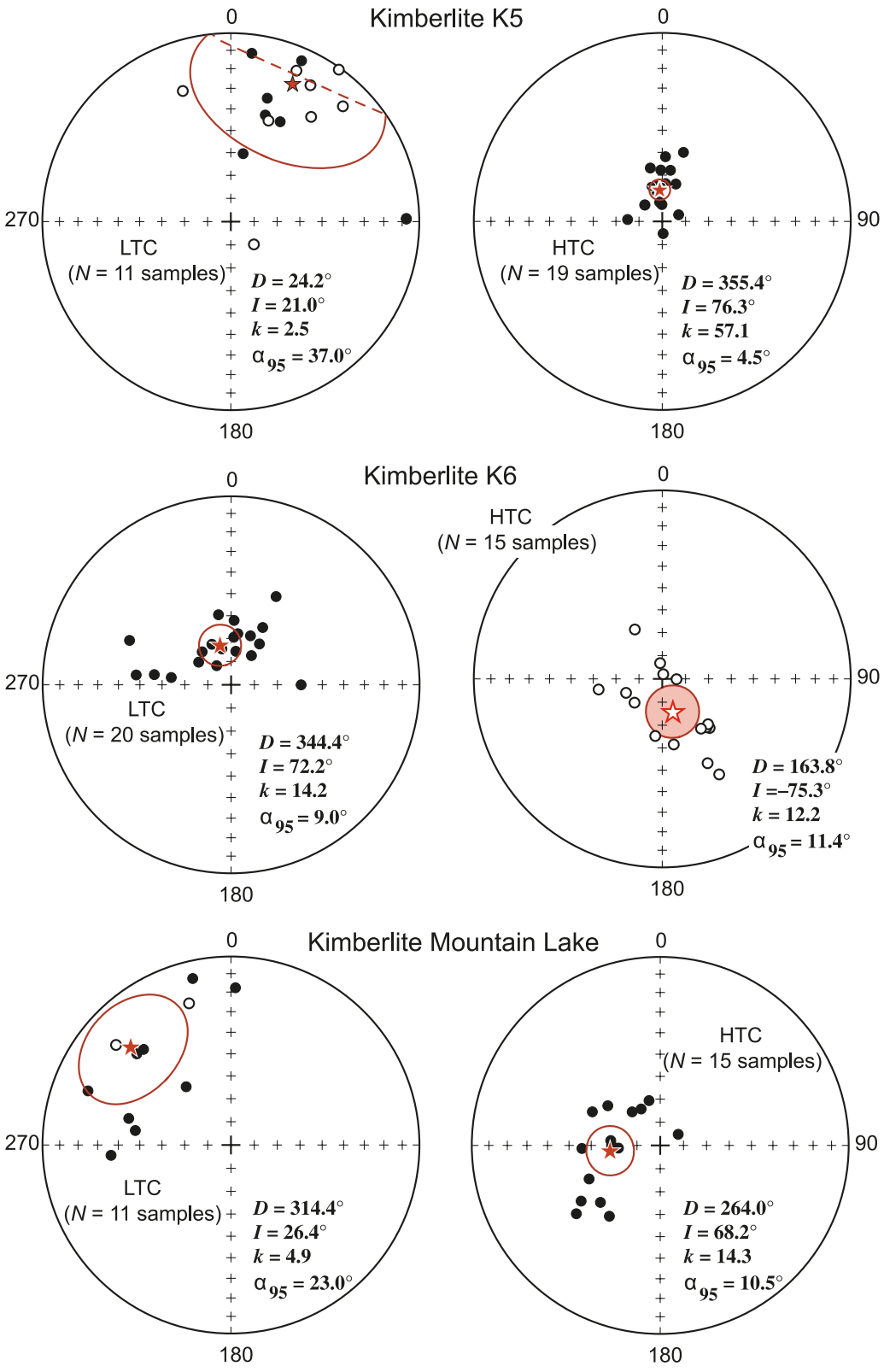

Table 2. Site-mean paleomagnetic directions for the low- and high-temperature components of magnetization of Alberta ultramafic bodies.

Ultramafic body	Component	Site latitude (°N)	Site longitude (°E)	*N*	*D* (°)	*I* (°)	*k*	α_{95} (°)	Notes
K5	LTC	56.89	244.36	11	24.2	21.0	2.5	37.0	11d
	HTC			19	355.4	76.3	57.1	4.5	19d
K6	LTC	56.91	244.40	20	344.4	72.2	14.2	9.0	20d
	HTC (directions and great circles together)			33	173.4	–70.7	10.9	7.9	15d 18c
	HTC (only directions)			15	163.8	–75.3	12.2	11.4	15d
Mountain Lake	LTC	55.45	242.28	11	314.4	26.4	4.9	23.0	11d
	LTC (after clockwise rotation for 70°)				24.4	26.4	4.9	23.0	11d
	HTC			15	264.0	68.2	14.3	10.5	15d
	HTC (after clockwise rotation for 70°)				334.0	68.2	14.3	10.5	15d

Note: LTC, Low-temperature (low-field) component, HTC, high-temperature (high-field) component; *N*, number of directions for samples accepted for calculation; *D* (*I*), declination (inclination) of characteristic component of NRM; *k*, α_{95}, precision parameter and half-angle radius of the 95% probability confidence cone. Entry d or c in Notes means number of directions and (or) great circles accepted for calculations; for example, 15d 18c means that 15 directions and 18 great circles were used for statistics to calculate the mean direction.

Fig. 8. Results of alternating field and thermal demagnetization for K6 kimberlite samples. See Fig. 6 legend for further details. NRM, natural remanent magnetization.

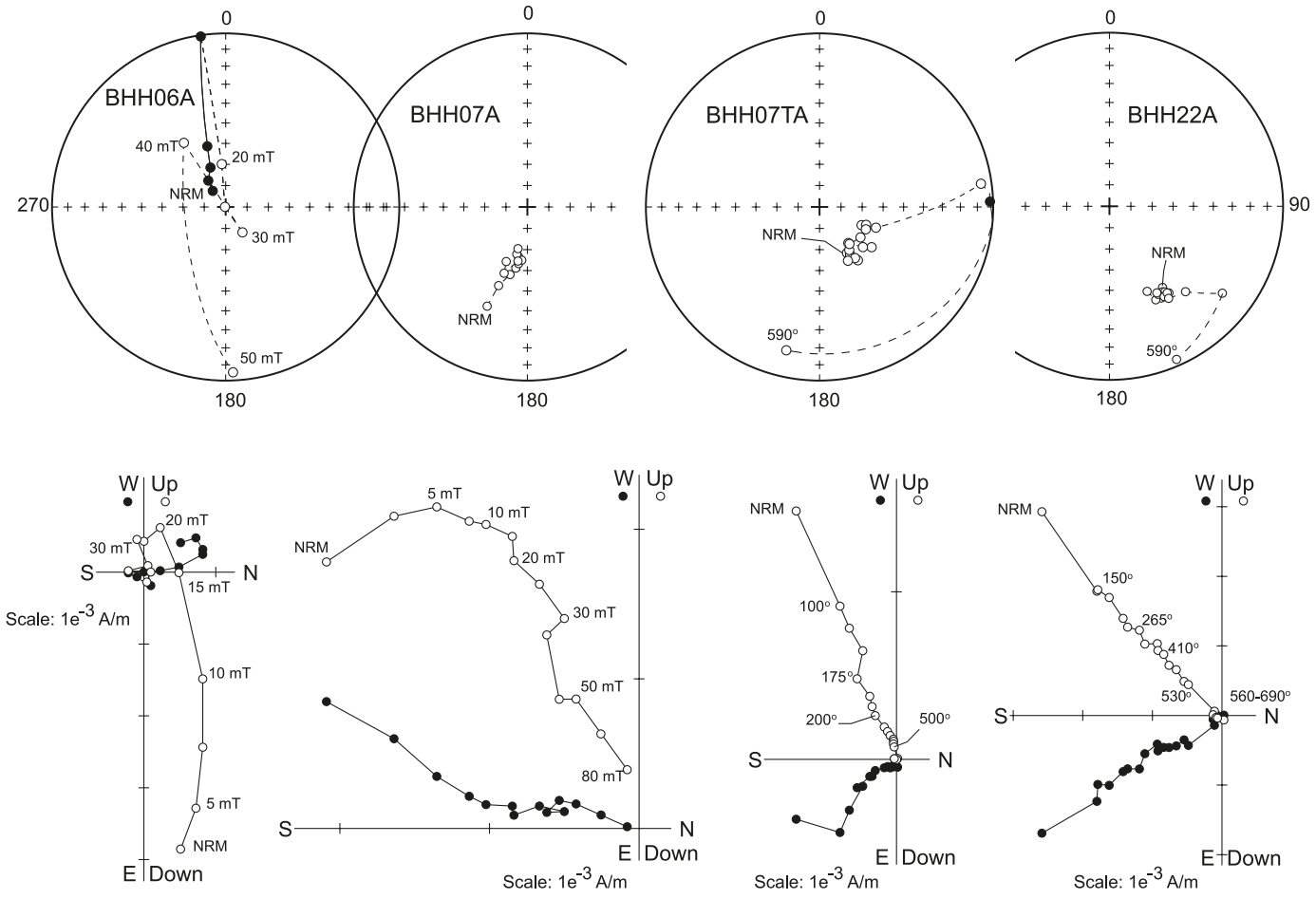

to determine whether the sandstone had normal or reversal polarity. The LTC temperature is weak and can be easily removed at 10 mT. The LTC directions for single samples are scattered and the mean value cannot be evaluated at this stage. The HTC always has negative inclinations and is quite dispersed in terms of declinations (the cause of the field orienting difficulty). Reversed polarity in the host sandstone close to the ultramafic body provides evidence that the area was not subject to "late" metamorphism, and the HTC directions are most likely primary. Some authors

Fig. 9. Results of alternating field and thermal demagnetization for Mountain Lake kimberlite samples. See Fig. 6 legend for further details. NRM, natural remanent magnetization.

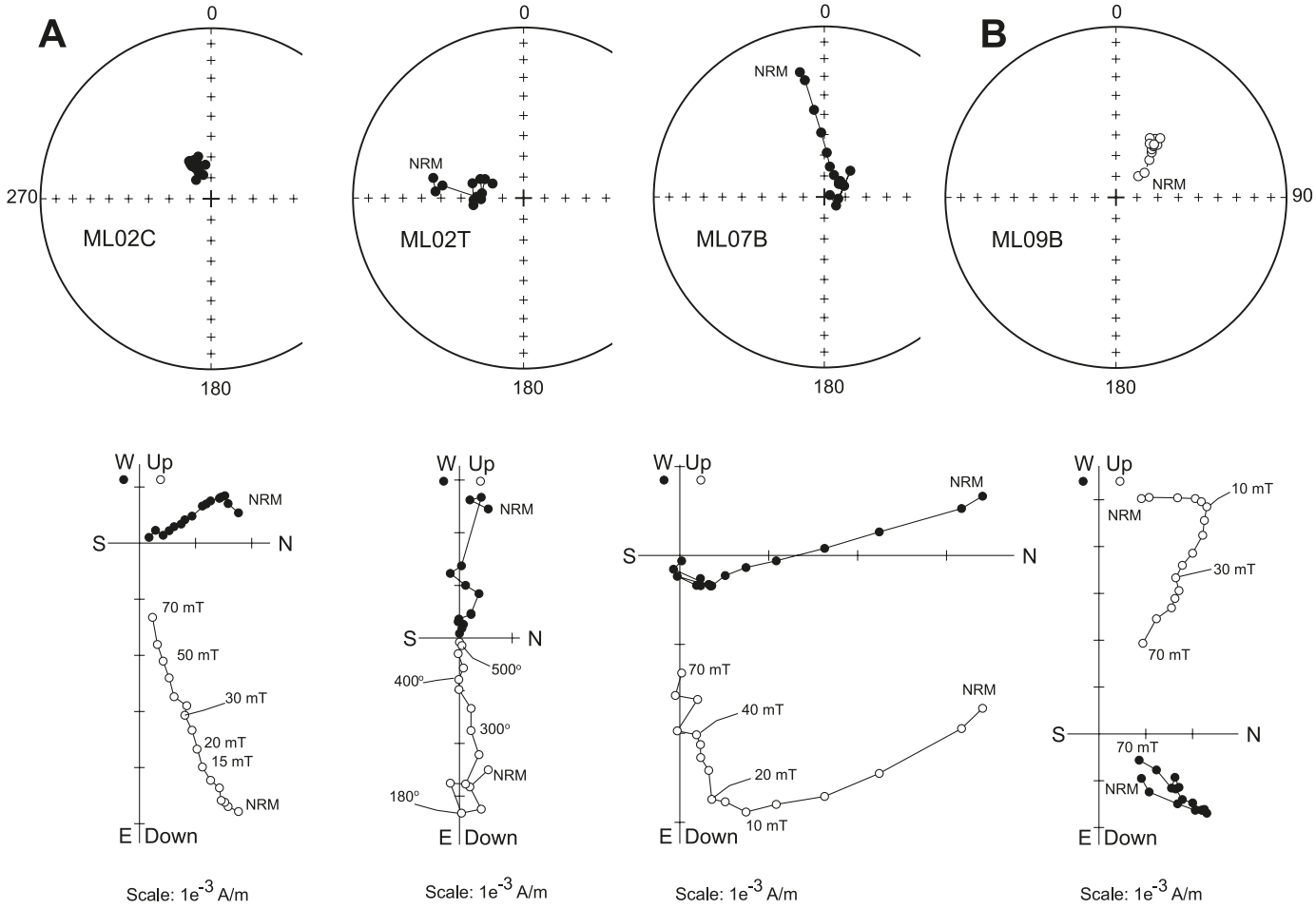

argue in favour of a "cold" emplacement temperature, which would limit the overprinting effects, but other cases of kimberlite-related remagnetization (thermochemical) can also occur (see the discussion on emplacement temperature regime in the introduction). Our study of the host Cretaceous sediments shows that Mountain Lake kimberlite emplacement occurred during a normal polarity interval and did not overprint the reverse polarity of the host sediments despite being directly adjacent to the intrusion. It may indicate that the margin had relatively low emplacement temperatures compared with the central part of the outcrop. Van Fossen and Kent (1993) demonstrated that the metamorphic effect did not extend much further than a width of the kimberlite body with relatively small size (a few metres). The ML body is much larger in size, and if the margins were cooler than the central part, sediments a few dozen metres away could avoid notable remagnetization.

McClelland and Erwin (2003) described a petromagnetic technique to evaluate the emplacement temperature for volcanoclastic rock. If magnetite is the main carrier of the remanent magnetization, then emplacement temperature in the clastic rock falls between the lowest and highest demagnetizing temperature. The primary magnetization of large inclusions (8–85 cm) could survive relatively low emplacement temperature (around 350 °C) and have scattered directions because of chaotic orientation of the clasts. The LTC acquired during emplacement of magma at ~350 °C would have the same direction for all samples. In our study, the LTC for all three kimberlite bodies was isolated between 150 and 200 °C. The samples do not have scattered HTC directions, i.e., most xenoliths have been remagnetized during the magma emplacement because of their relatively small size and may have higher than 300–350 °C emplacement temperatures, remagnetizing all inclusions in the studied samples.

Discussion

The paleomagnetic analysis completed here enabled us to calculate the paleomagnetic poles for K5, K6, and Mountain Lake ultramafic bodies (Fig. 10; Table 3). For comparative purposes, the North American apparent polar wander path (APWP) from Besse and Courtillot (2002) is also shown with average poles at 5 million year intervals. Due to the complex APWP pattern for North America and because of overlapping confidence cones for individual poles, it is problematic to establish an exact paleomagnetic age in the Cretaceous. The opening of the North Atlantic defined North America's predominant displacement in a mostly west-northwest orientation. The distance to the North geographic

Fig. 10. Equal-area projection of paleomagnetic poles from K5, K6, and Mountain Lake kimberlites obtained in the present study (from Table 3) with their 95% confidence ellipses (shadow areas). Grey dots are the North American apparent polar wander path (APWP) from Besse and Courtillot (2002) with some ages indicated in Ma. Target APWP reference poles at 85 and 90 Ma are highlighted with larger circles and numbers; their confidence ellipses are darker too. Study poles are shown as large black circles. ML-2 signifies the ML pole after 70° hypothetical clockwise rotation of the Mountain Lake area relative to Buffalo Head Hills.

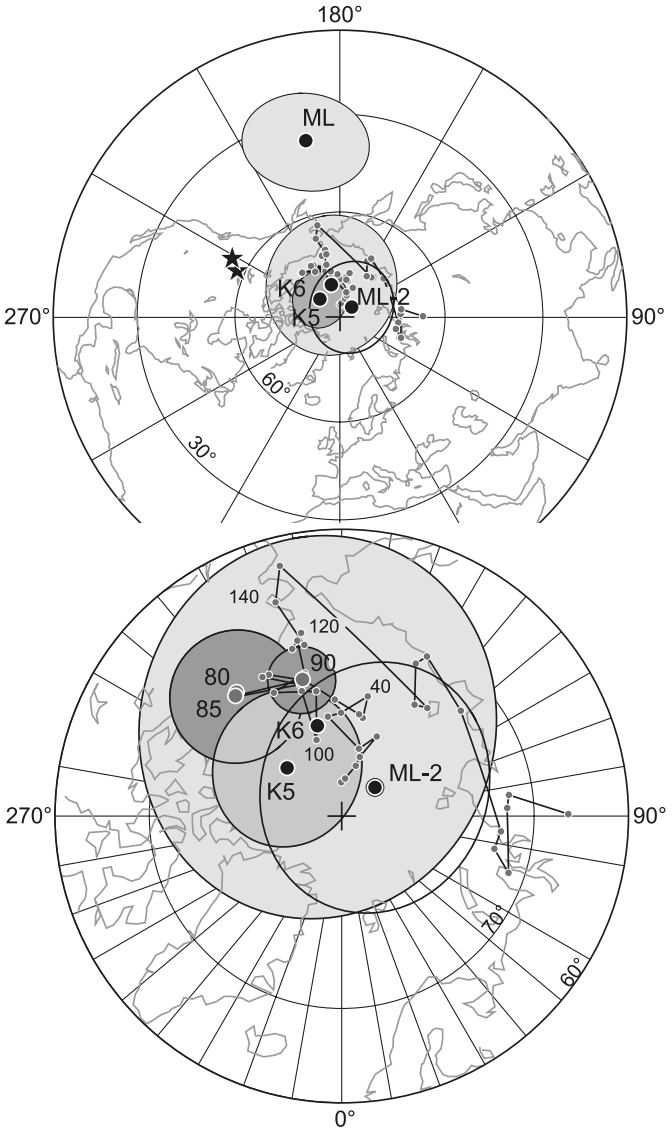

pole remained virtually steady, which considerably reduces the precision of paleomagnetic dating for this time interval. However, using additional information on geomagnetic polarity and published palynology and absolute dates (Table 4), a range of possible ages can be determined.

The U–Pb perovskite emplacement age for the K5 kimberlite corresponds to 87.6 ± 4.6 Ma (Skelton et al. 2003; Heaman et al. 2004; Eccles et al. 2008). The paleomagnetic pole for K5 (Table 3) fits with a number of Late Cretaceous North American poles including reference poles at 85 and 90 Ma based on overlapping confidence intervals (Fig. 10). The high-temperature component has positive inclinations that confirm kimberlite eruption occurred during the Cretaceous superlong normal polarity interval. The polarity scale of Cande and Kent (1995) sets an upper limit for the interval at 83 Ma. Reference poles older than 90 Ma are clustered and cannot be separated in terms of significance of their confidence intervals (see Besse and Courtillot 2002) so that we have to rely on absolute dating to determine a lower age limit. These results narrow the paleomagnetic age of the K5 kimberlite to an interval from ~90 Ma to exactly 83 Ma.

We calculated the paleomagnetic pole for the K6 kimberlite using the mean obtained with only directions (Table 3). The paleomagnetic pole corresponds to the broad range of the North American reference poles (Fig. 10) intersecting with all Late Cretaceous poles in the terms of confidence interval. The "approximate" (i.e., not recommended) radiogenic U–Pb perovskite date is 91.9 ± 2 Ma (Eccles 2004), which falls on the Cretaceous normal polarity long interval. The HTC from this study has reverse polarity and, therefore, cannot be of ca. 92 Ma age. A younger age interval of between 83.0 and 79.075 Ma better corresponds to the reverse polarity interval and is the authors' recommendation for a revised K6 emplacement age (Fig. 11). The K6 pole is situated fairly close to the expected 80 Ma position (73.5°N, 221.4°E). Less likely younger ages could fall into reverse polarity intervals of 71.071–68.737 Ma, 73.619–73.374 Ma, 73.291–73.004 Ma, and 71.587–71.338 Ma. We suspect a younger age is unlikely given the Late Cretaceous (Coniacian to Campanian) radiogenic age of the majority of the Buffalo Head Hills ultramafic bodies.

We consider the paleomagnetic pole for the Mountain Lake ultramafic body as preliminary (Table 3). Due to the incoherence between the Mesozoic part of the APWP and the paleomagnetic pole, an exact paleomagnetic age cannot be specified at this stage of the study (Fig. 11). The reason could be related to the fractured nature of the exposed rock surface and, thus, the problematic core orientation. Secondly, ML may have intruded during a period of polarity reversal so that the geomagnetic field might not be coherent to the expected axial dipole field. Alternative explanation involves hypothetical 70° tectonic rotation of the Mountain Lake area relatively to Buffalo Head Hills (a clockwise rotation of the LTC transfers to the anticlockwise relative tectonic rotation of the ML area). Such rotation would bring the notable difference between the ML pole and APWP to a reasonable quantity when circles of confidence of the ML pole and 80 Ma North American pole overlap each other to a certain extent (see pole ML-2 in Fig. 10). Possible tectonic causes for such post-Late Cretaceous rotation are mentioned in the "ML paleomagnetic" section.

Despite the complexity of the obtained pole interpretation, the Mountain Lake samples have positive inclinations of HTC allowing us to put some constraints on the age of the ultramafic body. Late Campanian sediments intercalated with the ultramafic rock have been dated between ~76 and 75 Ma (Leckie et al. 1997). Our study showed that the sandstone hosting ML has reverse polarity and, therefore, should not be older than 83 Ma (the upper border of the normal polarity Cretaceous superchron). In addition, the Mountain Lake kimberlite has normal polarity, suggesting that emplacement cannot be younger than 79.075 Ma (the upper

Table 3. Paleomagnetic poles calculated during this study.

		Site coordinates (°)		Paleomagnetic pole coordinates (°)			
	Ultramafic body	Latitude (N)	Longitude (E)	Latitude (N)	Longitude (E)	dp/dm (°)	*N*
1	K5	56.89	244.36	82.5	228.7	7.7/8.3	19
2	K6 (directions and circles together)	56.91	244.40	85.5	129.9	11.9/13.4	33
	K6 (only directions)			80.2	194.6	19.1/20.1	15
3*	Mountain Lake	55.45	242.28	37.3	190.9	14.9/17.7	15
	Mountain Lake after clockwise rotation of the HTC for 70°			74.1	148.0	14.9/17.7	15

Note: dp/dm, semiaxes of the 95% confidence ellipsoid of paleomagnetic pole; *N*, number of samples used to determine pole.
*preliminary result.

Table 4. Summary of the dates for selected ultramafic bodies in northern Alberta.

	Ultramafic body	Depth (m)	Age (Ma)	Dating method	Reference
1	K5	N/A	87±3	U–Pb perovskite	Skelton et al. (2003); Heaman et al. (2004); Eccles et al. (2008)
		Surface	~90–83	Paleomagnetism	This study
2	K6	Surface	91.9±2	U–Pb perovskite	Eccles (2004)
		Surface	<83 (most likely 83.0–79.075)	Paleomagnetism	This study
3	Mountain Lake sediments	In the adjacent creek	83.0–79.075	Paleomagnetism	This study
4	Mountain Lake	Clasts	68	Palynology	Wood et al. (1998)
		Various depths laminated sediments	76–75	Palynology	Leckie et al. (1997)
		N/A	78±9 to 74±7	AFT (central age)	Leckie et al. (1997)
		N/A	72±7	AFT (central age)	Leckie et al. (1997)
		Surface	<79.075	Paleomagnetism	This study

Note: AFT, apatite fission track.

Fig. 11. Geomagnetic polarity time scale for an interval 95–65 Ma from Cande and Kent (1995). Arrows denote the age for the reversal polarity intervals. Paleomagnetic age constraints determined in this study and radiogenic and palynological age constraints from other works are given as age ranges for the K5, K6, and Mountain Lake (ML) kimberlite bodies.

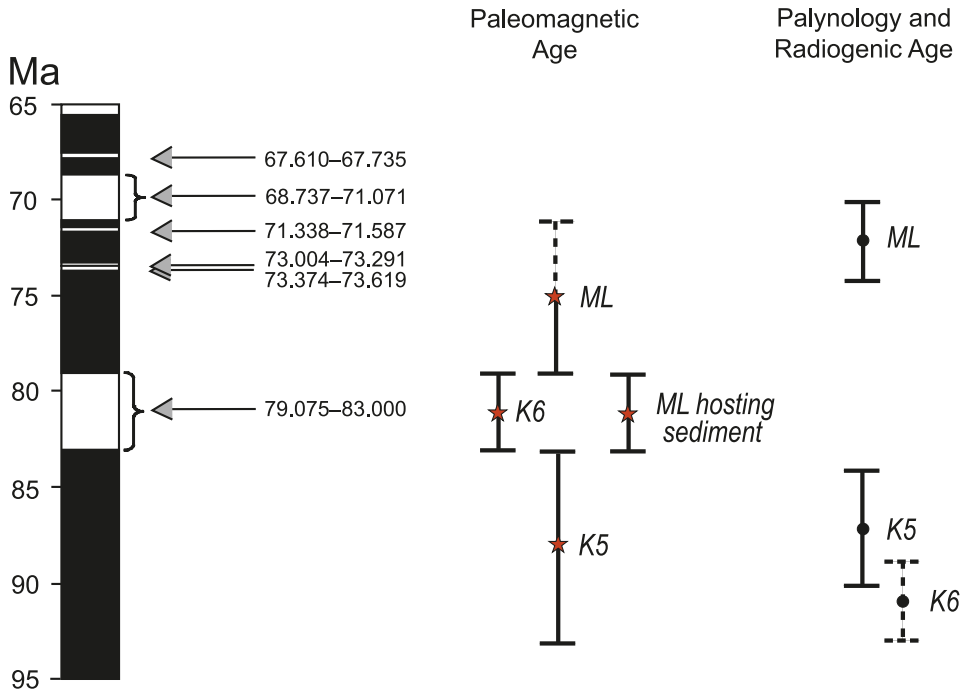

boundary of the reverse polarity interval). These constraints place the host sediment age in the narrow intervals of reverse polarity (83.000–79.075 Ma, 73.619–73.374 Ma, 73.291–73.004 Ma, and 71.587–71.338 Ma). Taking in consideration the palynology and absolute dates from the ML kimberlite (see Table 4) we consider the interval of 83–79.075 Ma to be most reasonable for the sediments because that is slightly older than the palynological and apatite fission track dates from the kimberlite. Therefore, the most probable age of the ML kimberlite should be regarded as younger than 79.075 Ma.

Acknowledgements

The paper benefitted enormously from the helpful comments and suggestions of H. Halls and P. McCausland. The authors also thank A. Mar from the Department of Chemistry for granted access to the Physical Property Measuring System. The study was accomplished with the financial support of the University of Alberta (Physics Department) start-up fund and the Natural Sciences and Engineering Research Council of Canada (NSERC) grant to V.K. The authors would also like to thank the Alberta Geological Survey for field work support and Ashton Mining of Canada Inc. (now Stornoway Diamonds Corp.) for permitting access to the ultramafic outcrops.

References

Armstrong, R.L. 1993. Late Triassic to Earliest Eocene magmatism in the North American Cordillera: implications for the Western Interior Basin. *In* Evolution of the Western Interior Basin. *Edited by* W.G.E. Caldwell and E.G. Kauffman. Geological Association of Canada, Special Paper 39, pp. 49–72.

Besse, J., and Courtillot, V. 2002. Apparent and true polar wander and the geometry of the geomagnetic field over the last 200 Myr. Journal of Geophysical Research, **107**:2300. doi:10.1029/2000JB000050.

Cande, S.C., and Kent, D.V. 1995. Revised calibration of the geomagnetic polarity timescale for the Late Cretaceous and Cenozoic. Journal of Geophysical Research, **100**(B4): 6093–6095. doi:10.1029/94JB03098.

Chen, D., and Olson, R. 2005. Regional stratigraphic framework of Buffalo Head Hills – Peerless Lake Region, northern Alberta. Alberta Energy and Utilities Board, EUB/AGS Earth Sciences Report 2005-05, 47 p.

Cogné, J.P. 2003. PaleoMac: a Macintosh™ application for treating paleomagnetic data and making plate reconstructions. Geochemistry Geophysics Geosystems, **4**(1): 1007. doi:10.1029/2001GC000227.

Dankers, P. 1981. Relationships between median destructive field and remanent coercive forces for dispersed natural magnetite, titanomagnetite, and hematite. Geophysical Journal of the Royal Astronomical Society, **64**: 447–461.

Dixon, G.R. 1993. Cretaceous tectonics and sedimentation in northwest Canada. *In* Evolution of the Western Interior Basin. *Edited by* W.G.E. Caldwell and E.G. Kauffman. Geological Association of Canada, Special Paper 39, pp. 119–129.

Dunlop, D.J. 2002. Theory and application of the Day plot (Mrs/Ms versus Hcr/Hc) 2. Application to data for rocks, sediments, and soils. Journal of Geophysical Research. Solid Earth, **107**(B3): 2057. doi:10.1029/2001JB000487.

Dunlop, D.J., and Özdemir, Ö. 1997. Rock magnetism. Cambridge University Press, New York, 573 p.

Eccles, D.R. 2004. Petrogenesis of the northern Alberta kimberlite province, M.Sc. Thesis, University of Alberta, Edmonton, Alta., 179 p.

Eccles, D.R., Pana, D.C., Paulen, R., and Olson, R.A. 2003. Geological Setting of the northern Alberta kimberlite province. *In* Slave Province and northern Alberta field trip guidebook. *Edited by* B.A. Kjarsgaard. Guidebook prepared for the 8th International Kimberlite Conference, Geological Survey of Canada, Miscellaneous Publication G-293.

Eccles, D.R., Heaman, L.M., Luth, R.W., and Creaser, R.A. 2004. Petrogenesis of the Late Cretaceous northern Alberta kimberlite province. Lithos, **76**: 435–459. doi:10.1016/j.lithos.2004.03.046.

Eccles, D.R., Creaser, R.A., Heaman, L.M., and Ward, J. 2008. Rb–Sr and U–Pb geochronology and setting of the Buffalo Head Hills kimberlite field, northern Alberta. Canadian Journal of Earth Sciences, **45**(5): 513–529. doi:10.1139/E07-050.

Fisher, R. 1953. Dispersion on a sphere. Proceedings of the Royal Society of London, Series A: Mathematical and Physical Sciences, **217**: 295–305. doi:10.1098/rspa.1953.0064.

Fontana, G., Mac Niocaill, C., Brown, R.J., Sparks, R.S.J., and Field, M. 2008. Emplacement Temperatures of Pyroclastic and Volcaniclastic Deposits in kimberlite Pipes in Southern Africa. *In* the 9th International Kimberlite Conference, Extended Abstract No. 9IKC-A-00259.

Halls, H.C. 1976. A least-squares method to find a remanence direction from converging remagnetization circles. Geophysical Journal of the Royal Astronomical Society, **45**: 297–304.

Hamilton, W.N., Langenberg, W.C., Price, M.C., and Chao, D.K. 1999. Geological map of Alberta. Alberta Geological Survey, Map 236, scale 1 : 1 000 000.

Heaman, L.M., Kjarsgaard, B.A., and Creaser, R.A. 2004. The temporal evolution of North American kimberlites. Lithos, **76**: 377–397. doi:10.1016/j.lithos.2004.03.047.

Jones, D.L. 1968. Paleomagnetism of Premier mine kimberlite. Journal of Geophysical Research, **73**(22): 6937–6945. doi:10.1029/JB073i022p06937.

Kirschvink, J.L. 1980. The least-squares line and plane and the analysis of paleomagnetic data. Geophysical Journal of the Royal Astronomical Society, **62**: 699–718.

Leckie, D.A., Kjarsgaard, B.A., Peirce, J.W., Grist, A.M., Collins, M., Sweet, A., et al. 1997. Geology of a Late Cretaceous possible kimberlite at Mountain Lake, Alberta – chemistry, petrology, indicator minerals, aeromagnetic signature, age, stratigraphic position and setting. Geological Survey of Canada, Open File Report 3441, 202 p.

Lockhart, G., Grutter, H., and Carlson, J. 2004. Temporal, geomagnetic and related attributes of kimberlite magmatism at Ekati, Northwest Territories, Canada. Lithos, **77**(1–4): 665–682. doi:10.1016/j.lithos.2004.03.029.

McClelland, E., and Erwin, P.S. 2003. Was a dacite dome implicated in the 9500 BP collapse of Mt. Ruapehu? A palaeomagnetic investigation. Bulletin of Volcanology, **65**: 294–305.

McFadden, P.L. 1977. A palaeomagnetic determination of the emplacement temperature of some South African kimberlites. Geophysical Journal of the Royal Astronomical Society, **50**: 605–619.

McFadden, P.L., and Jones, D.L. 1977. Paleomagnetism of some Upper Cretaceous kimberlite occurrences in South Africa. Earth and Planetary Science Letters, **34**(1): 125–135. doi:10.1016/0012-821X(77)90113-3.

McFadden, P.L., andMcElhinny, M.W. 1988. The combined analysis of remagnetization circles and direct observations in paleomagnetism. Earth and Planetary Science Letters, **87**: 161–172.

Mitchell, R.H. 1986. Kimberlites: Mineralogy, Geochemistry, and Petrology. Plenum Press, New York, 442 p.

Price, R.A. 1994. Cordilleran tectonics and the evolution of the Western Canada Sedimentary Basin. *In* Geological Atlas of the Western Sedimentary Basin. *Edited by* G.D. Mossop and I. Shetsen. Canadian Society of Petroleum Geologists and Alberta Research Council, Calgary, Alta., pp.13–24.

Ross, G.M., Broome, J., and Miles, W. 1994. Potential Fields and Basement Structure — Western Canada Sedimentary Basin. *In* Geological Atlas of the Western Canadian Sedimentary Basin. *Edited by* G.D. Mossop and I. Shetson. Canadian Society of Petroleum Geologists and Alberta Research Council, Calgary, Alta., pp. 41–48.

Skelton, D., Clements, B., McCandles, T.E., Hood, C., Aulbach, S., Davies, R., and Boyer, L.P. 2003. The Buffalo Head Hills Kimberlite Province, Alberta. *In* 8th International Kimberlite Conference, Slave Province and northern Alberta field trip guidebook. *Edited by* B.A. Kjarsgaard, pp. 11–19.

Skinner, E.M.W., and Marsh, J.S. 2004. Distinct kimberlite pipe classes with contrasting eruption processes. Lithos, **76**: 183–200. doi:10.1016/j.lithos.2004.03.044.

Stripp, G.R., Field, M., Schumacher, J.C., and Sparks, R.S.J. 2006. Post-emplacement serpentinization and related hydrothermal metamorphism in a kimberlite from Venetia, South Africa. Journal of Metamorphic Geology, **24**: 515–534. doi:10.1111/j.1525-1314.2006.00652.x.

Van Fossen, M.C., and Kent, D. 1993. A palaeomagnetic study of 143 Ma kimberlite dikes in central New York State. Geophysical Journal International, **113**: 175–185. doi:10.1111/j.1365-246X.1993.tb02538.x.

Watson, K.D. 1967. Kimberlites of Eastern North America. *In* Ultramafic and Related Rocks. *Edited by* P.J. Wyllie. John Wiley & Sons, Inc., New York, pp. 312–323.

Wood, B.D., Scott Smith, B.H., and de Gasparis, S. 1998. The Mountain Lake kimberlitic pipes of Northwest Alberta: exploration, geology and emplacement model. *In* 7th International Kimberlite Conference, Extended Abstracts, Cape Town, South Africa. *Edited by* J.J. Gurney, J.L. Gurney, M.D. Pascoe and S.H. Richardson. Red Roof Design cc, South Africa, pp. 960–962.

Wynne, P.J., Irving, E., Schulze, D.L., Hall, D.C., and Helmstaedt, H.H. 1992. Paleomagnetism and age of three Canadian Rocky Mountain diatremes. Canadian Journal of Earth Sciences, **29**(1): 35–47. doi:10.1139/e92-005.

Zijderveld, J.D.A. 1967. AC demagnetization of rocks, analysis of results. *In* Methods in Paleomagnetism. *Edited by* D.W. Collinson, K.M. Creer and S.K. Runcorn. Elsevier, Amsterdam, The Netherlands, pp. 254–286.